

Neutron Vibrational Spectroscopic Study of the Acetylene:Ammonia (1:1) Cocrystal Relevant to Titan, Saturn's Moon

Morgan J. Kramer,^a Benjamin A. Trump,^b Luke L. Daemen,^c Rafael Balderas-Xicohtencatl,^c Yongqiang Cheng,^c Anibal J. Ramirez-Cuesta,^c Craig M. Brown,^{b,d} Tomče Runčevski^{a*}

a Department of Chemistry, Southern Methodist University, Dallas, TX 75275 (USA) E-mail: truncevski@smu.edu

b National Institute of Standards and Technology, Center for Neutron Research, Gaithersburg, MD 20899 (USA)

c Oak Ridge National Laboratory, Oak Ridge, TN 37830 (USA)

d Department of Chemical and Biomolecular Engineering, University of Delaware, DE 19716 (USA)

ABSTRACT: The surface of Titan, Saturn's icy moon, is believed to be comprised of various molecular minerals with a great diversity in structure and composition. Under the surface conditions, 93 K and 1.45 atm, most small molecules solidify and form minerals, including acetylene and ammonia. These two compounds can form single-component solids but also a 1:1 binary cocrystal that exhibits intriguing rotor phase behavior. This cocrystal is a putative mineral on Titan and other planetary bodies such as comets. In addition, the structure of the cocrystal is relevant to fundamental science as it can help better understand the emergence of rotor phases. Here we present a detailed vibrational neutron spectroscopic study supported by neutron powder diffraction study on the cocrystal and the single-phase solids. The experimentally observed spectral bands were assigned based on theoretical calculations. The established spectra-properties correlations for the cocrystal corroborate the observed properties. To the best of our knowledge, this study presents the first example of the application of neutron vibrational spectroscopy in studying Titan-relevant organic minerals.

INTRODUCTION

In 2019, NASA announced the New Frontiers Mission to Saturn's icy moon, Titan. A rotorcraft named Dragonfly is scheduled for launch in 2027, with arrival on the moon expected in the 2030s.¹ This endeavor closely follows the Cassini-Huygens mission (1997-2017), which was vital in exploring Saturn and its moons.² It is no surprise that Titan remains a focal point of scientific interest, as it is the only planetary body in the Solar System, apart from Earth, to possess a dense and chemically active atmosphere that is rich with organic compounds derived from methane and nitrogen.³ On Titan, these compounds can react in the upper atmosphere primarily via photochemical reactions induced by solar radiation and charged particles originating from Saturn's magnetosphere.⁴ This ionizing radiation causes methane and nitrogen to dissociate and form reactive species that interact to form organic molecules ranging from very simple (ethane, propane, acetylene, etc.) to very complex molecules (>10,000 Da) that precipitate onto Titan's surface. Chemical reactions can continue even on the surface,⁵ further contributing to the remarkable compositional diversity of this environment. Under Titan's surface conditions (≈ 90 K– 94 K and ≈ 1.5 bar), methane is close to its triple point, and ethane (and propane) exists as a liquid comprising the vast lakes and seas.⁶ All larger organics are expected to exist as solids under these conditions. These chemicals also dissolve in the

hydrocarbon lakes, with modest to poor solubility.⁷ Similar to the hydrological cycle on Earth, Titan has a seasonal cycling of evaporation and precipitation of the hydrocarbon lakes, producing evaporite lakebeds and deposits of organic minerals akin to evaporate deposits on Earth.⁷ This combination of chemical and physical processes leads to the formation of solid surfaces with extraordinary complexity in composition and structure. In light of the forthcoming Dragonfly mission, as well as to further our fundamental knowledge of the physical chemistry of the smallest organic molecules, it is imperative to gain a better understanding of these systems.

Acetylene and ammonia are some of the smallest and most fundamental organic molecules in the universe and are found in relatively large quantities on Titan. In fact, acetylene is one of the most abundant organic products generated in Titan's atmosphere.⁸ Its presence was detected in the upper atmosphere by Voyager 1, and later confirmed during the Cassini-Huygens mission by its numerous instruments, including Cassini composite infrared spectrometer (CIRS),⁸ ion and neutral mass spectrometer (INMS),⁹ and gas chromatograph mass spectrometer (GCMS).¹⁰ Acetylene has a relatively high solubility in liquid alkanes and is also known to form cocrystals with numerous organic co-components.¹¹ Ammonia and ammonium were also detected in the upper atmosphere of Titan by the Cassini INMS instrument. Further studies indicate that Titan's mantle may be

comprised of as much as 1.6 mass percent to 10.7 mass percent NH_3 resulting from Titan's extensive subsurface $\text{NH}_3\text{-H}_2\text{O}$ ocean.¹² Ammonia or ammonium on Titan's surface would likely originate from the advection of melt pockets, transport by microporous clathrate grains, explosive cryovolcano eruptions, or local geysering from NH_3 -rich deposits in the crust.¹²⁻¹⁵ The coexistence of these two materials, coupled with their ability to interact and form cocrystals is suggestive of the possibility that acetylene:ammonia cocrystals are abundant organic minerals on the landscape of Titan. Furthermore, these binary solids are also relevant in the studies of other planetary bodies. For example, both materials have been detected as constituents of the comets, such as Hyakutake.¹⁶ Both molecules are also believed to be present in prebiotic Earth.¹⁷⁻¹⁹ The intermolecular interactions within condensed phases of such simple organic systems can be relevant for the studies of planetary bodies and as well as modeling of processes occurring on young prebiotic Earth. Such interactions are indeed strong between ammonia and acetylene,²¹⁻²² resulting in a stable 1:1 cocrystal that was reported in 2009.²³ In the last ten years, there have been various studies focused on this cocrystal under Titan's conditions, particularly using infrared (IR) and Raman vibrational spectroscopic studies.^{24, 25} The synthesis and formation of the acetylene:ammonia (1:1) cocrystal has been extensively studied by *in-situ* Raman spectroscopy, and vibrational modes corresponding to lattice vibrations and the C-H bends of acetylene have been frequently used as diagnostic signals for cocrystal formation.²¹⁻²⁴ These signals had relatively large blue shifts in the cocrystal of 5.24 meV (42.3 cm^{-1}) and 8.16 meV (65.8 cm^{-1}) respectively, when compared to the single component spectra. These large shifts in the Raman spectra were particularly useful as a probe for the presence of this cocrystal and this was used as a marker for both the formation and degradation of the material under liquid methane and ethane. Infrared spectroscopy has also been used to characterize the cocrystal in core-shelled aerosolized particles.²⁵ We aimed to expand our understanding of the vibrational fingerprint of this cocrystal through the use of NVS as the concluding piece of its spectroscopic characterization.

IR and Raman spectroscopy have specific symmetry-dependent selection rules for vibrational modes – certain modes are only IR active, whereas others are Raman active. On the contrary, neutron vibrational spectroscopy (NVS) is a far more comprehensive tool for studying the vibrational structure of materials, as it detects all vibrational modes, regardless of symmetry. Furthermore, neutrons interact with the strong nuclear force of the atomic nucleus, as opposed to the electron cloud probed by photons in optical measurements. The particle-particle interactions are particularly strong with H/D atoms. Considering the hydrogen-rich environment on Titan, NVS presents an excellent tool for the exploration of hydrogen-rich putative Titanian minerals and condensed phases relevant to young prebiotic Earth. Finally, NVS can typically access vibrational frequencies in the phonon range (5 meV-25 meV; 40 cm^{-1} - 200 cm^{-1}) with much higher resolution than other vibrational methods. This spectral region contains valuable information on the lattice vibrations and structure of the material.

To the best of our knowledge, NVS has not been applied in the study of Titan-relevant organic minerals, and there are scarce reports on the application of the method in planetary research.²⁰⁻²⁵ Here we report a detailed NVS study of the acetylene:ammonia (1:1) cocrystal. To prove that the spectroscopic data have

been collected from the target material, we have simultaneously collected and analyzed Time-of-Flight Neutron Powder Diffraction (TOF-NPD) data. Finally, we have complemented the experimental studies with theoretical calculations, which allowed for detailed spectral assignments and structure-properties correlations. The spectroscopic results provide important insights into the structure, composition, and properties of a putative Titanian mineral.

EXPERIMENTAL

Neutron Vibrational Spectroscopy. Data collection was performed on VISION (BL-16B) the neutron vibrational spectrometer at the Spallation Neutron Source (SNS) at Oak Ridge National Laboratory.²⁶ The cocrystal was formed *in situ* via a 1:1 stoichiometric condensation of ammonia and acetylene. Ammonia and acetylene gases were added in equal volumes to the sample can and allowed to mix for 10 minutes before the can was crash cooled to 77 K. The vessel was then slowly cooled to 5 K over 2.5 hrs before data was collected. Measurements of NVS and TOF-NPD were collected in tandem at (5, 50, 75, 93, 125, 150, and 175) K with 1-hr thermal equilibrations allowed between steps. Upon reaching 175 K, the samples were allowed to slowly cool back to 5 K under the same increments and NVS and TOF-NPD were collected.

Time-of-Flight Neutron Powder Diffraction (TOF-NPD). Data collection was performed on VISION (BL-16B) the neutron vibrational spectrometer at the Spallation Neutron Source (SNS) at Oak Ridge National Laboratory. TOF-NPD patterns were collected in tandem with NVS measurements, as described above.

Diffraction Data Analysis. TOF-NPD data were analyzed using the GSAS-II software package.²⁷ Space group, atomic and lattice parameters were taken from the literature for each phase. Specifically, *Aeam* for acetylene,²⁸ *P2₁3* for ammonia,²⁹ and *Ima2* for the acetylene:ammonia (1:1) cocrystal.²³ Precise lattice parameters, peak shapes, and background function were determined by Pawley refinement.³⁰

Computational Studies. Density Functional Theory (DFT) modeling was performed using the Vienna Ab initio Simulation Package (VASP).³¹ The calculation used Projector Augmented Wave (PAW) method.^{32, 33} The optB86b-vdW functional^{34, 35} with dispersion corrections was applied. The energy cutoff was 800 eV for the plane-wave basis of the valence electrons. The total energy tolerance for electronic energy minimization was 10^{-8} eV, and for structure optimization, it was 10^{-7} eV. The maximum interatomic force after relaxation was below $0.002\text{ eV}/\text{\AA}$. The lattice parameters and atomic coordinates measured in this work were used as the initial structure. Structural relaxation was first performed on the ions only (with the lattice constants fixed at the experimental values), after which full relaxation of the cell was performed. The vibrational eigenfrequencies and modes were then calculated by solving the force constants and dynamical matrix using Phonopy.³⁶ The OCLIMAX software³⁷ was used to convert the DFT-calculated phonon results to the simulated INS spectra.

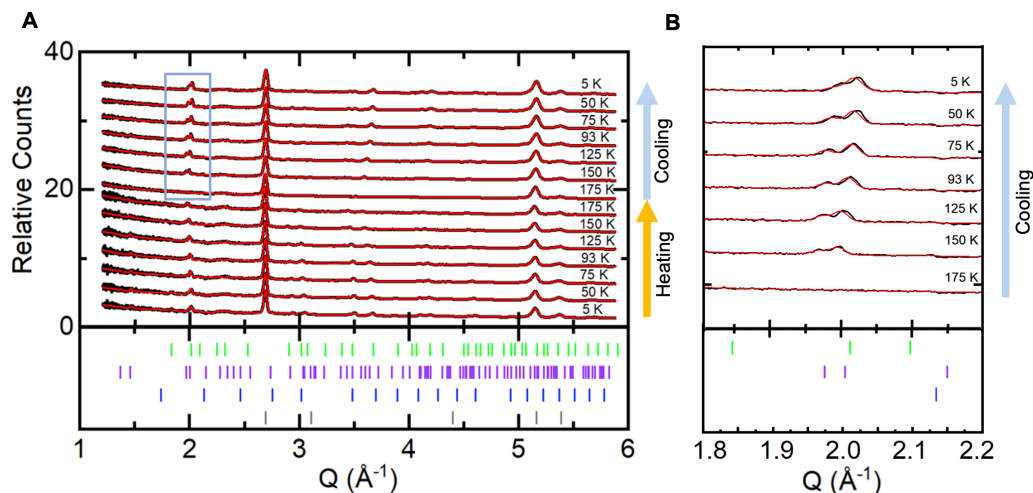


Figure 1. (A) TOF-NPD patterns (black line) and Pawley fits (red trace) for diffraction data collected at various temperatures. The direction of heating is from bottom to top. (B) $Q = 1.8\text{--}2.2 \text{ \AA}^{-1}$ range of Pawley fits for the region highlighted in blue. Tick marks refer to reflection from the cocrystal between acetylene and ammonia (purple), the reactants ammonia (blue), acetylene (green), as well as aluminum (grey).

RESULTS & DISCUSSION

The acetylene:ammonia (1:1) cocrystal was synthesized by condensation and crystallization of equimolar amounts of ammonia and acetylene gas at ambient pressure. To confirm the synthesis of the cocrystal and to obtain information about the crystal structure and stoichiometry of the solid, we collected and analyzed TOF-NPD data simultaneously while collecting the NVS data. Figure 1A presents diffraction patterns for a 1:1 molar combination of ammonia and acetylene collected at variable temperatures upon heating of a crash-cooled sample from 5 K to 175 K and later slowly cooled again to 5 K. The diffraction data were analyzed by Pawley fitting against the reported unit cell parameters of the acetylene:ammonia (1:1) cocrystal, as well as molecular crystalline ammonia and molecular crystalline acetylene (aluminum metal was added to account for the Bragg reflections from the canister).

The analysis of the crashed-cooled sample clearly shows reflection from the 1:1 cocrystal, whose crystal structure is described in the *Iam2* space group.²³ Figure 1B shows a region of the pattern containing coherent scattering from Bragg peaks of the cocrystal ((2 0 0) and (2 1 1) reflections), whose intensities grow as a function of cooling. The cocrystal is presumably the thermodynamically most stable phase at low temperature and ambient pressure. However, due to kinetic effects and experimental limitations such as imperfect mixing and fast cooling, certain amounts of unreacted ammonia and acetylene can be expected in the sample as molecular solids and have been observed in Figure 1. This situation is frequently observed in the synthesis of numerous cocrystals.²³⁻²⁶

Upon gradual heating to 150 K, a characteristic thermal expansion is observed by a shift of the diffraction maxima to lower Q values on heating (Figure 1A) and higher Q values upon cooling (Figure 1B). This observation is consistent with the previously reported large and anisotropic thermal expansion of the cocrystal.²⁴ The thermal expansion continues upon heating to 150 K, after which the cocrystal incongruently melts into solid

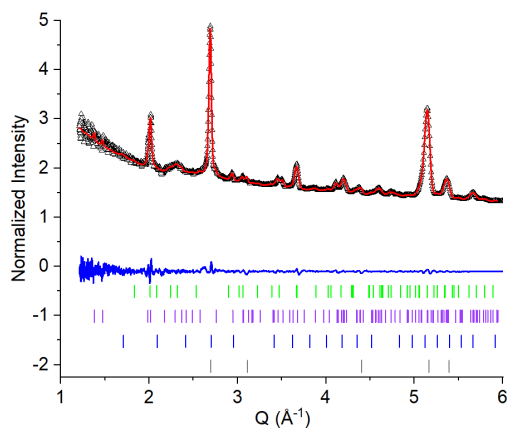


Figure 2. Pawley fit for TOF-NPD measurements of acetylene-ammonia mixture slow cooled down to $T = 5 \text{ K}$ (left). Data shown as black triangles, refinement in red, background in light grey, and difference curve in dark grey. From bottom to top, tick marks refer ammonia (blue), acetylene (green), and acetylene-ammonia cocrystal (purple). Fit statistics for this refinement was $R_{wp} = 0.963\%$, GOF: 1.553. Symbols are larger than or commensurate with error which represent $\pm 1\sigma$.

ammonia and a liquid mixture of ammonia and acetylene.²⁴ Subsequent slow cooling of the mixed liquid revealed the same processes in reverse order (Figure 1), resulting in crystallization of the organic phases. It can be expected that the mechanism of the cocrystal formation is driven by a peritectic transition of solid ammonia and liquid acetylene, similar to other reported solids.²⁴ However, concurrent crystallization of all phases is also a possibility when considering several other potential contributions. First, the melting points of ammonia and acetylene

□

are in close proximity (195.4 and 192.3 K, respectively), with a $\Delta T = 3.1$ K. Second, there is a possibility of the formation of a supercooled liquid that later crystallizes. Third, the formation of crystals from any phase can seed the nucleation of other organic phases in the phase mixture.

Molecular crystalline ammonia and acetylene, for single-component systems, are the thermodynamically most stable forms for each individual component. However, in a perfectly miscible binary mixture that features the formation of a cocrystal, three crystalline solids—the cocrystal, ammonia, acetylene—cannot coexist as three thermodynamically most stable phases. All but one of these phases, depending on the conditions, must be thermodynamically metastable. The observed coexistence of molecular solids and a cocrystal results from kinetic effects. The observation of kinetic effects, with trapping of metastable phases at low temperatures, can have implications on the formation of the mineralogical makeup of the Titanian surface. Kinetic trapping of metastable minerals has been observed on Earth (e.g., cristobalite, a quenched high-temperature phase of silica) and has been hypothesized for molecular minerals on Titan (e.g., a quenched high-temperature phase of acetonitrile).⁴⁰ The occurrence of such metastable solids in this binary system showcases the complexity of the phase equilibria that can exist in higher-component mixed systems. Titan, in essence, is an extremely complicated mixture at a planetary scale. Therefore, various kinetically trapped phases must be considered in the modeling of the mineralogical makeup.

Figure 3 presents the NVS data collected as a function of heating of a crash-cooled sample (the spectroscopic data was collected simultaneously with the TOF-NPD patterns presented in Figure 1). The NVS spectra had a clear temperature dependence, where strong vibrational signals were observed at low temperatures as a result of lower thermal vibrations. Upon heating, the peak intensity decreased, and the broadness of the signals increased. The pronounced sensitivity of the NVS spectral bands on thermal vibrations is limiting to the application of this method in studies of the formation (crystallization) and melting

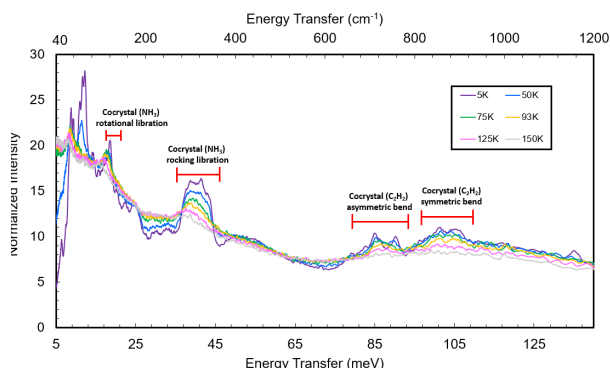


Figure 3. Variable Temperature NVS spectra overlay of the acetylene:ammonia (1:1) cocrystal mixture with peak assignments. The vibrational spectra were collected in tandem with diffraction patterns upon heating up from the crash-cooled sample at 5 K. Exact ranges for assigned peaks can be found in Table 1.

(fusion) of the cocrystal, which both happen at high temperatures. This observation exemplifies the advantage of using tandem NVS-Raman or NVS-IR approaches in detailed studies of these systems considering the robustness of Raman or IR towards thermal vibrations. However, at low temperatures, the NVS spectrum offers a comprehensive representation of the vibration modes including the phonon region.

Figure 4 presents an overlay of the NVS spectra at 5 K of the cocrystal prepared via crash cooling and the cocrystal prepared by heating and slow cooling of the sample. Expectedly, both spectra contain vibrational peaks from the cocrystal; however, both spectra have features that correspond to both the starting materials and the cocrystal. For example, the ammonia rotational libration from the neat crystal can be seen from 28 meV to 35 meV (225 cm^{-1} to 283 cm^{-1}). Upon heating and subsequent cooling of the sample to 5 K, most of these features disappear.

Table 1 presents a list of the observed vibrations for the cocrystal and their assignments. Spectral assignments were done based on DFT theoretical calculations that resulted in a simulation of the spectra, shown in Figure 5. There is a good agreement between experiment and simulation in the overall profile of the spectra, which allows us to assign the peaks to the corresponding vibrational modes. For some of the vibrational modes, the peak positions (i.e., the calculated and measured frequencies) agree well, but for some other modes, especially the rotational libration of ammonia at around 10 meV, the calculated frequencies are somewhat higher. This is not surprising because the larger H displacements associated with the librational modes often lead to anharmonicity (while the calculation was performed under the harmonic approximation).

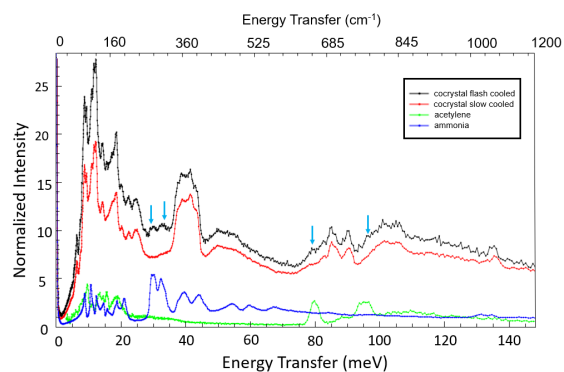


Figure 4. Overlay of two methods of synthesizing the acetylene:ammonia (1:1) cocrystal and their neat components. Crash cooled (black) and slow cool from 175 K down to 5 K (red). Blue arrows indicate features from solid ammonia and acetylene in the cocrystal NVS spectrum.

□

Table 1. List of experimental and computed energy transfers for the assigned vibrational modes of the acetylene:ammonia (1:1) cocrystal at 5K compared to the neat cocrystal components of acetylene and ammonia.

		Neutron Vibrational Spectroscopy					
molecule	vibrational mode	Pure Component		(1:1) Acetylene:Ammonia Cocrystal			
		Energy Transfer (cm ⁻¹)	Energy Transfer (meV)	Energy Transfer (cm ⁻¹)	Energy Transfer (meV)	?? (cm ⁻¹)	?? (meV)
acetylene	lattice vibrations	<200	<25	<200	<25	-	-
	C ₂ H ₂ asymmetric bending	645	80	660 to 750	82 to 93	16 to 105	2 to 13
	C ₂ H ₂ symmetric bending	766	95	766 to 887	95 to 110	0 to 121	0 to 15
ammonia	lattice vibrations	<200	<25	<200	<25	-	-
	NH ₃ rotational libration	225 to 283	28 to 35	73 to 105	9 to 13	153 to 77	-19 to -22
	NH ₃ rocking libration	298 to 379	37 to 47	290 to 363	36 to 45	8 to 16	-1 to -2
	Overtone of rotational libration + NH ₃ rocking libration	403 to 564	50 to 70	-	-	-	-
	NH ₃ umbrella bend	1048 to 1088	130 to 135	1088	135	-40 to 0	-5 to 0

Pure component shifts for acetylene were gathered from the literature.⁴¹ Ammonia and cocrystal values are reported as measured on VISION. Negative values of $\Delta\nu$ indicate a red shift (lower frequency) and positive values indicate a blue shift (higher frequency) in the cocrystal when compared to the bare component vibrations.

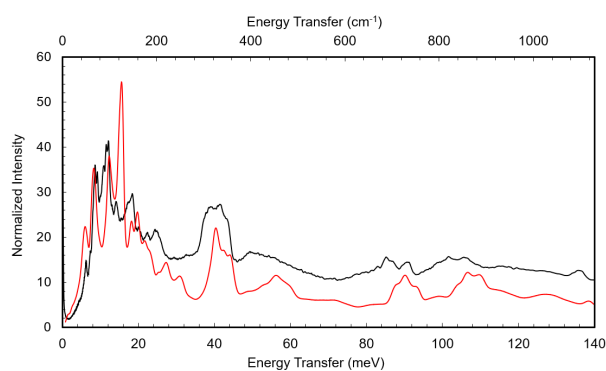


Figure 5. Experimentally observed NVS spectrum (black) of the acetylene:ammonia (1:1) cocrystal overlaid with computationally predicted NVS spectrum from the partially (ion only) relaxed structure (red)

Molecular crystals, especially those comprised of small organic molecules, often feature properties such as colossal and anisotropic thermal expansion,²⁴ plasticity (rotor phases),³⁸ and similar macroscopic properties that originate from their unique crystal packing and bonding. Changes in intermolecular interactions within the crystal packing can have major implications on the physical properties. For example, in the crystal structure of solid ammonia (Figure 6A) there is a continuous network of strong N-H hydrogen bonding, with N-H \cdots N bond distances of 2.556(4) Å and N to N interatomic distances of 3.947(7) Å. As such, this crystal structure is not prone to dynamic disorder and does not exhibit plasticity. On the other hand, acetylene relies primarily on π - π and weak hydrogen π -cloud interactions as the main interaction within the crystal structure (Figure 6B). Nonetheless, presumably due to the geometrical simplicity of the molecule, this structure also does not exhibit plasticity. Interestingly, the 1:1 cocrystal shows pronounced dynamic disorder and plasticity.^{38,39} The cocrystal has hydrogen bonding interactions between the ammonia nitrogen center and the acetylene C-H bond. The NH \cdots N hydrogen bonding interaction is stronger in the cocrystal than in the bare ammonia structure demonstrated by its shorter intermolecular C-H \cdots N distance of

2.538(2) Å. The ammonia molecules within this packing rotate on picosecond time scales.³⁸ The dramatic change in the hydrogen bonding environment in the single-component solids vs. 1:1 cocrystal is also expected to be manifested in the NVS spectra with pronounced shifts in the energy of the phonon and vibrational modes.

Comparison of the vibration modes of ammonia in the hydrogen-bonded structure in the single-component crystal vs. the more “loosely” packed environment in the 1:1 cocrystal corroborates the emergence of a rotor phase. In the molecular solid, the N-H \cdots N hydrogen bonding interaction is strong, thus resulting in an energy transfer for the rotational libration mode to be relatively high energy, detected at 28 meV - 35 meV (225 cm⁻¹ - 293 cm⁻¹) in the NVS spectra. This change in the energy of the vibration can be attributed to a few factors that are elucidated by the crystal structures shown in Figure 6. In the cocrystal, the four strong hydrogen bonding interactions in solid ammonia are

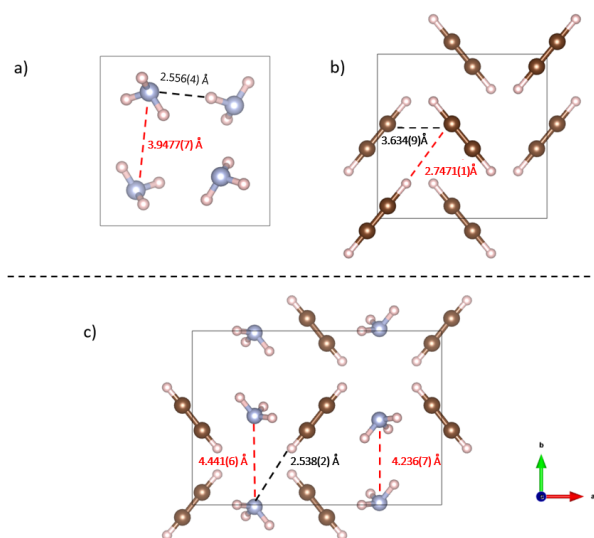


Figure 6. Crystal structures and selected bond distances of a) ammonia, *P213*, b) acetylene, *Aeam*, c) acetylene:ammonia (1:1) cocrystal, *Iam2*. (Color legend: blue = nitrogen, brown = carbon, off-white = hydrogen).

□

disrupted and replaced by two hydrogen bonding interactions between the acetylene C-H as the hydrogen bonding donor, with the nitrogen lone pair from ammonia as the hydrogen bonding acceptor. Importantly, this bonding puts almost no restriction to the NH₃ rotational libration, which is very different from the N-H···N hydrogen bonding that “locks” the three “legs” of the NH₃ molecule in the ammonia crystal. In the neat NH₃ crystal, there is a strong hydrogen bonding interaction between the adjacent NH₃ molecules. As the peritectic reaction between ammonia and acetylene proceeds, the lattice expands in order to incorporate the acetylene molecule. The acetylene:ammonia (1:1) cocrystal orients in a chain-like manner,²³ where each C-H bond of acetylene behaves as a hydrogen bond donor to the neighboring ammonia molecules. Effectively, the incorporation of acetylene into the ammonia lattice results in the displacement of the previously established N-H···N interaction with much stronger hydrogen bond donor, as reflected in their distinct pK_a values, 32.5 for NH₃ and 25 for C₂H₂ and thereby contributing to the shorter C-H···N hydrogen bond length. As a result, the same NH₃ rotational libration in the acetylene:ammonia (1:1) cocrystal is now dramatically red-shifted and is detected at 9 meV to 13 meV (73 cm⁻¹ to 105 cm⁻¹) with a colossal $\Delta\nu$ of 19 meV to 22 meV (153 cm⁻¹ to 177 cm⁻¹).

Two other peaks originating from ammonia also have appreciable red-shifts in the NVS spectra when comparing the neat crystals to the acetylene:ammonia (1:1) cocrystal. Namely, the NH₃ rocking libration, which was observed at 36 meV to 45 meV (290 cm⁻¹ to 363 cm⁻¹), and the NH₃ umbrella bend seen at 135 meV (1088 cm⁻¹) in the neat crystal of ammonia. Both peaks had a modest red-shift associated with the cocrystal formation. The NH₃ rocking libration was modestly redshifted by 1 meV to 2 meV (8 cm⁻¹ to 16 cm⁻¹), and the NH₃ umbrella bend was redshifted up to 5 meV (40 cm⁻¹). These redshifts of NH₃ vibrational modes are again a result of the less restrictive hydrogen bonding network and packing environment in the cocrystal, compared to the neat ammonia crystal, although they are less dramatic than the NH₃ rotational libration.

Other characteristic shifts observed in the NVS spectrum of the cocrystal arise from the C₂H₂ symmetric and asymmetric bending. The acetylene asymmetric bending mode in the neat acetylene crystal has an expected energy transfer of 80 meV (645 cm⁻¹). In the cocrystal, this mode is observed from 82 meV to 93 meV (660 cm⁻¹ to 750 cm⁻¹) representing an overall blue shift of this vibration of 2 meV to 13 meV (16 cm⁻¹ - 105 cm⁻¹). For the acetylene symmetric bending, the neat acetylene crystal has this mode predicted and observed at 95 meV (766 cm⁻¹). This acetylene symmetric bending has a similar blue shift associated with the cocrystal formation, where now this bend is observed between 95 meV to 110 meV (766 cm⁻¹ - 887 cm⁻¹) corresponding to an overall shift of 0 meV to 15 meV (0 cm⁻¹ to 121 cm⁻¹). These blueshifts of the bending modes can be explained by the C-H···N hydrogen bond which is perpendicular to the C-H bond in the acetylene molecule and is thus along the direction of the bending motion.

CONCLUSIONS

In summary, here we have presented a detailed NVS, TOF-NPD and theoretical study of the acetylene:ammonia (1:1) cocrystal that is a putative organic mineral on Titan, comets, and potentially other planetary bodies. First, the synthesis, structure, and

phase composition of the cocrystal were confirmed by Pawley fitting analyses of TOF-NPD patterns, collected in tandem with the spectroscopic data. The crystallographic data have revealed that the cocrystal is the major phase in the system, but measurable amounts of the single-component reactant solids have also been detected due to kinetic effects during the synthesis of the cocrystal. The spectral assignment of the vibrational modes observed in the NVS data was done based on DFT modeling. Colossal shifts have been detected in the cocrystal, compared to the single-component solids. Most notably, the NH₃ rotational libration in the cocrystal was found to be dramatically red-shifted to lower energies. This shift results from the breaking up the strong hydrogen bonding environment of the bare ammonia structure and replacing the four sets of hydrogen donor/acceptor pairs and replacing them with two C-H···N interactions. This results in a less rigidly bound NH₃ unit which can more readily rotate. The shift to lower energies and a weaker hydrogen bonding environment corroborates the previously observed plastic (rotor) behavior of the cocrystal. Other ammonia peaks also had appreciable red-shifts, including the NH₃ rocking libration and the NH₃ umbrella bend. Characteristic shifts of the C₂H₂ molecule were observed with its symmetric and asymmetric bending. Overall, the established spectra-properties correlations for the cocrystal corroborate the observed structural and macroscopic properties. To the best of our knowledge, this study presents the first example of the application of neutron vibrational spectroscopy in the study of Titan-relevant organic minerals. Having no symmetry selection rules, and being extremely sensitive to hydrogen atoms, NVS is an excellent method for the study of hydrocarbon and molecular solids as putative minerals on Titan.

ASSOCIATED CONTENT

Supporting Information

This material is available free of charge via the Internet at <http://pubs.acs.org>.

ACKNOWLEDGMENTS

This material is based upon work supported by the National Science Foundation under Grant No. 2143581. This research was funded, in part, by the Robert A. Welch Foundation under Grant No. N-2012-20220331, and the American Chemical Society Petroleum Research Fund. The TOC was designed with contributions from high school students (ESI). A portion of this research used resources at the Spallation Neutron Source, a DOE Office of Science User Facility operated by the Oak Ridge National Laboratory (ORNL). Computing resources were made available through the VirtuES and the ICE-MAN projects, funded by the Laboratory Directed Research and Development program and Compute and Data Environment for Science (CADES) at ORNL

REFERENCES

- 1) “NASA’s Dragonfly Will Fly Around Titan Looking for Origins, Signs of Life” NASA Press Release 19-052, June 27, 2019.

- 2) a) Titan from Cassini-Huygens, Brown, R.H.; Lebreton, J.P.; Waite, J.H. Springer, Heidelberg, **2009**; b) Niemann, H.B.; Atreya, S.K.; Bauer, S.J.; Carignan, G.R.; Demick, J.E.; Frost, R.L.; Gautier, D.; Haberman, J.A.; Harpold, D.N.; Hunten, D.M.; Israel, G.; Lunine, J.I.; Kasprzak, W.T.; Owen, T.C.; Paulkovich, M.; Raulin, F.; Raen, E.; and Way, S.E. *Nature*, **2005**, 438, 779-784; c) Coustenis, A.; Hirtzig, M. *Res. Astron. Astrophys.*, **2009**, 9, 249-268.
- 3) a) S. Gupta, E. Ochiai and C. Ponnampereuma, *Nature* **1981**, 293, 752-727; b) R. D. Lorenz, C. P. McKay and J. I. Lunin, *Science*, **1997**, 275, 642-644.
- 4) a) Krasnopolsky, V.A. *Icarus* **2009**, 201, 226-256; b) Vuitton, V.; Yelle, R. V.; Cui, J. *J. Geo. Res. Planets*, **2008**, 113, E05007; c) Molina-Cuberos, G. J.; Schwingschuh, K.; López-Moreno, J. J.; Rodrigo, R.; Lara, L.M.; and Anicich, V. *J. Geo. Res. Planets*, **2002**, 107, 9-1-9-11
- 5) Abplanalp, M. L.; Frigge, R.; and Kaiser, R.I. *Science Adv.* **2019**, 5, eaaw5841.
- 6) Coustenis, A.; Achterberg, R. K.; Conrath, B. J.; Jennings, D. E.; Marten, A.; Gautier, D.; Nixon, C. A.; Flasar, F. M.; Teanby, N. A.; B?zard, B.; Samuelson, R. E.; Carlson, R. C.; Lellouch, E.; Bjoraker, G. L.; Romani, P. N.; Taylor, F. W.; Irwin, P. G. J.; Fouchet, T.; Hubert, A.; Orton, G. S.; Kunde, V. G.; Vinatier, S.; Mondellini, J.; Abbas, M. M.; Courtin, R. The Composition of Titan's Stratosphere from Cassini/CIRS Mid-Infrared Spectra. *Icarus* **2007**, 189 (1), 35– 62
- 7) a) Glein, C. R.; Shock, E. L. A Geochemical Model of Non-Ideal Solutions in the Methane-Ethane-Propane-Nitrogen-Acetylene System on Titan. *Geochim. Cosmochim. Acta* **2013**, 115, 217– 240. b) Singh, S.; Combe, J.-P.; Cordier, D.; Wagner, A.; Chevrier, V. F.; McMahon, Z. Experimental Determination of Acetylene and Ethylene Solubility in Liquid Methane and Ethane: Implications to Titan's Surface. *Geochim. Cosmochim. Acta* **2017**, 208, 86– 101. c) Hazen, R.M. Titan Mineralogy: A window on organic mineral evolution. *American Mineralogist*. **2018**, 103 (3), 341-342. d) Maynard-Casely, H.E., Cable, M.L., Malaska, M.J., Vu, T.H., Choukroun, M., and Hodyss, R. Prospects for mineralogy on Titan. *American Mineralogist*, **2018**, 103, 343–349.
- 8) Waite, J. H.; Niemann, H.; Yelle, R. V.; Kasprzak, W. T.; Cravens, T. E.; Luhmann, J. G.; McNutt, R. L.; Ip, W.-H.; Gell, D.; De La Haye, V.; Müller-Wordag, I.; Magee, B.; Borggren, N.; Ledvina, S.; Fletcher, G.; Walter, E.; Miller, R.; Scherer, S.; Thorpe, R.; Xu, J.; Block, B.; Arnett, K. Ion Neutral Mass Spectrometer Results from the First Flyby of Titan. *Science*. **2005**, 308 (5724).
- 9) Gupta, S.; Ochiai, E.; Ponnampereuma, C. Organic Synthesis in the Atmosphere of Titan. *Nature* **1981**, 293 (5835), 725– 727.
- 10) Niemann, H. B.; Atreya, S. K.; Demick, J. E.; Gautier, D.; Haberman, J. A.; Harpold, D. N.; Kasprzak, W. T.; Lunine, J. I.; Owen, T. C.; Raulin, F. Composition of Titan's Lower Atmosphere and Simple Surface Volatiles as Measured by the Cassini-Huygens Probe Gas Chromatograph Mass Spectrometer Experiment. *J. Geophys.*
- 11) Boese, R. Co-Crystals with Acetylene: Small Is Not Simple!. *Chem. - Eur. J.* **2010**, 16 (7), 2131– 2146.
- 12) Lopes, R. M. C.; Mitchell, K. L.; Stofan, E. R.; Lunine, J. I.; Lorenz, R.; *et al.* Cryovolcanic Features on Titan's Surface as Revealed by the Cassini Titan Radar Mapper. *Icarus* **2007**, 186 (2), 395– 412. b) Sotin, C.; Jaumann, R.; Buratti, B. J.; Brown, R. H.; *et al.* Release of Volatiles from a Possible Cryovolcano from near-Infrared Imaging of Titan. *Nature* **2005**, 435 (7043), 786– 789. c) Lunine, J. I. Does Titan have an ocean? A review of current understanding of Titan's surface. *Rev. Geophys.* **1993**, 31, 133–149. d)
- 13) Wall, S. D.; Lopes, R. M. C.; Stofan, E. R.; Wood, C. A.; Radebaugh, J. L.; Horst, S. M.; Stiles, B. W.; Nelson, R. M.; Kamp, L. W.; Janssen, M. A.; Lorenz, R. D.; Lunine, J. I.; Farr, T. G.; Mitri, G.; Paillou, P.; Paganelli, F.; Mitchell, K. L. Cassini RADAR Images at Hotei Arcus and Western Xanadu, Titan: Evidence for Geologically Recent Cryovolcanic Activit. *Geophys. Res. Lett.* **2009**, 36, L04203.
- 14) Gilliam, A. E.; Lerman, A. Formation Mechanisms of Channels on Titan through Dissolution by Ammonium Sulfate and Erosion by Liquid Ammonia and Ethane. *Planet. Space Sci.* **2016**, 132, 13– 22.
- 15) a) Lorenz, R. D. Pillow Lava on Titan: Expectations and Constraints on Cryovolcanic Processes. *Planet. Space Sci.* **1996**, 44 (9), 1021– 1028. b) Sotin, C.; Tobie, G. Internal Structure and Dynamics of the Large Icy Satellites. *C. R. Phys.* **2004**, 5 (7), 769– 780. c) Fortes, A. D.; Grindrod, P. M.; Trickett, S. K.; Vočadlo, L. Ammonium Sulfate on Titan: Possible Origin and Role in Cryovolcanism. *Icarus* **2007**, 188 (1), 139– 153.
- 16) a) Brooke, T. Y.; Tokunaga, A.T.; Weaver, H.A.; Crovisier, J.; Bockelée-Morvan, D.; Crisp, D. Detection of acetylene in the infrared spectrum of comet Hyakutake. *Nature*, **1996**, 383, 606-608. b) Biver, N.; Bockelée-Morvan, D.; Crovisier, J. *et al.* Chemical Composition Diversity Among 24 Comets Observed At Radio Wavelengths. *Earth Moon Planet.* **2002**, 90, 323–333. c) Biver, N.; Bockelée-Morvan, D.; Crovisier, J. *et al.*, 'Spectroscopic Monitoring of Comet C/1996 B2 (Hyakutake) with the JCMT and IRAM Radio Telescopes', *Astron. J.* **1999**, 118, 1850–1872.
- 17) Lorenz, R. D.; Mitchell, K. L.; Kirk, R. L.; Hayes, A. G.; Aharonson, O.; Zebker, H. A.; Paillou, P.; Radebaugh, J.; Lunine, J. I.; Janssen, M. A.; Wall, S. D.; Lopes, R. M.; Stiles, B.; Ostro, S.; Mitri, G.; Stofan, E. R. Titan's Inventory of Organic Surface Materials. *Geophys. Res. Lett.* **2008**, 35 (2)
- 18) Diederich, P.; Geisberger, T.; Yan, Y.; Seitz, C.; Ruf, A.; Huber, C.; Hertkorn, N.; Schmitt-Kopplin, P. Formation, stabilization and fate of acetaldehyde and higher aldehydes in an autonomously changing prebiotic system emerging from acetylene. *Commun. Chem.* **2023**, 6, 38
- 19) Willacy, K.; Allen, M.; Yung, Y. A New Astrobiological Model of the Atmosphere of Titan. *Astrophys. J.* **2016**, 829 (2), 79
- 20) a) Parker, S. F.; Lennon, D.; Albers, P. W. Vibrational Spectroscopy with Neutrons: A Review of New Directions. *Appl. Spectrosc.* **2011**, 65 (12), 1325– 1341. b) Parker, S. F.; Ramirez-Cuesta, A. J.; Daemen, L.

□

- Vibrational Spectroscopy with Neutrons: Recent Developments. *Spectrochim. Acta - Part A Mol. Biomol. Spectrosc.* **2018**, 190, 518–523. c) Mitchell, P.; Parker, S.; Ramirez-Cuesta, A.; Tomkinson, J. *Vibrational Spectroscopy With Neutrons: With Applications in Chemistry, Biology, Materials Science and Catalysis*; World Scientific: Singapore, **2005**.
- 21) a) Hilpert, G.; Fraser, G. T.; Pine, A. S. Vibrational Couplings and Energy Flow in Complexes of NH₃ with HCN, HCCH, and HCCCCH. *J. Chem. Phys.* **1996**, 105, 6183–6191. b) Fraser, G. T.; Leopold, K. R.; Klemperer, W. The Structure of NH₃-Acetylene. *J. Chem. Phys.* **1984**, 80 (4), 1423–1426.
 - 22) Liu, Y.; Suhm, M. A.; Botschwina, P.; Fusina, L.; Schmatz, S.; Stoll, H.; Bak, K. L.; Stanton, J. F. Supersonic Jet FTIR and Quantum Chemical Investigations of Ammonia/acetylene Clusters. *Phys. Chem. Chem. Phys.* **2004**, 6 (19), 4642–4651.
 - 23) a) Boese, R.; Bläser, D.; Jansen, G. Synthesis and Theoretical Characterization of an Acetylene-Ammonia Co-crystal. *J. Am. Chem. Soc.* **2009**, 131 (6), 2104–2106. b) Boese, R. Co-Crystals with Acetylene: Small Is Not Simple!. *Chem. - Eur. J.* **2010**, 16 (7), 2131–2146.
 - 24) a) Cable, M. L.; Vu, T. H.; Maynard-Casely, H. E.; Choukroun, M.; Hodyss, R. The Acetylene-Ammonia Co-Crystal on Titan. *ACS Earth Sp. Chem.* **2018**, 2 (4), 366–375. b) Vu, T. H.; Cable, M. L.; Choukroun, M.; Hodyss, R.; Beauchamp, P. Formation of a New Benzene-Ethane Co-Crystalline Structure under Cryogenic Conditions. *J. Phys. Chem. A* **2014**, 118 (23), 4087–4094. c) Maynard-Casely, H. E.; Cable, M. L.; Malaska, M. J.; Vu, T. H.; Choukroun, M.; Hodyss, R. Prospects for Mineralogy on Titan. *Am. Mineral.* **2018**, 103 (3), 343–349. d) Cable, M. L.; Vu, T. H.; Malaska, M. J.; Maynard-Casely, H. E.; Choukroun, M.; Hodyss, R. A Co-Crystal between Acetylene and Butane: A Potentially Ubiquitous Molecular Mineral on Titan. *ACS Earth Sp. Chem.* **2019**, 3 (12), 2808–2815. e) Cable, M. L.; Runčevski, T.; Maynard-Casely, H. E.; Vu, T. H.; Hodyss, R. Titan in a Test Tube: Organic Co-Crystals and Implications for Titan Mineralogy. *Acc. Chem. Res.* **2021**, 54, 3050–3059. f) McConville, C. A.; Tao, Y.; Evans, H. A.; Trump, B. A.; Lefton, J. B.; Xu, W.; Yakovenko, A. A.; Kraka, E.; Brown, C. M.; Runčevski, T. Peritectic phase transition of benzene and acetonitrile into a cocrystal relevant to Titan, Saturn's Moon. *Chem. Comm.* **2020**, 56, 13520–13523
 - 25) Preston, T. C.; Signorell, R. The Formation and Stability of Co-Crystalline NH₃-C₂H₂ Aerosol Particles. *Mol. Phys.* **2012**, 110 (21–22), 2807–2815.
 - 26) Seeger, P.A.; Daemen L.L.; and Larese, J.Z.; Nuclear Instruments and Methods in Physics Research Section A, **2009** Volume 604, Issue 3, p. 719.
 - 27) Toby, B. H.; Von Dreele, R. B. GSAS-II: The Genesis of a Modern Open-Source All Purpose Crystallography Software Package. *J. Appl. Crystallogr.* **2013**, 46 (2), 544–549
 - 28) a) Koski, H. K.; Sándor, E. Neutron Powder Diffraction Study of the Low-Temperature Phase of Solid Acetylene-d 2. *Acta Crystallogr. Sect. B Struct. Crystallogr. Cryst. Chem.* **1975**, 31 (2), 350–353. b) Koski, H. K. The Structure of Solid Acetylene- d 2 , C 2 D 2 , at 4.2 K. A Further Refinement. *Acta Crystallogr. Sect. B Struct. Crystallogr. Cryst. Chem.* **1975**, 31 (3), 933–935.
 - 29) a) Olovsson, I.; Templeton, D. H. X-Ray Study of Solid Ammonia. *Acta Crystallogr.* **1959**, 12 (11), 832–836. b) Boese, R.; Niederprüm, N.; Bläser, D.; Maulitz, A.; Antipin, M. Y.; Mallinson, P. R. Single-Crystal Structure and Electron Density Distribution of Ammonia at 160 K on the Basis of X-Ray Diffraction Data. *J. Phys. Chem. B* **1997**, 101 (30), 5794–5799. c) Natta, G.; Casazza, E. No Title. *Gazzeta Chim. Ital.* **1930**, 60, 851.
 - 30) Pawley, G. S. Unit-Cell Refinement from Powder Diffraction Scans. *J. Appl. Crystallogr.* **1981**, 14 (6), 357–361.
 - 31) Kresse, G.; Furthmüller, J. Efficient iterative schemes for ab initio total-energy calculations using a plane-wave basis set. *Phys. Rev. B*, **1996**, 54, 11169–11186.
 - 32) Blochl, P. E. Projector augmented-wave method. *Phys. Rev. B*, **1994**, 50, 17953–17979.
 - 33) Kresse, G. & Joubert, D. From ultrasoft pseudopotentials to the projector augmented-wave method. *Phys. Rev. B*, **1999**, 59, 1758–1775.
 - 34) Perdew, J. P.; Burke, K.; Ernzerhof, M. Generalized gradient approximation made simple. *Phys. Rev. Lett.*, **1996**, 77, 3865–3868.
 - 35) Klimeš, J., Bowler, D. R. & Michaelides, A. Chemical accuracy for the van der Waals density functional. *J. Phys.: Cond. Matt.* **2010**, 22, 022201.
 - 36) Togo, A. & Tanaka, I. First principles phonon calculations in materials science. *Scr. Mater.*, **2015** 108, 1–5.
 - 37) Y. Q. Cheng, L. L. Daemen, A. I. Kolesnikov, A. J. Ramirez-Cuesta, *J. Chem. Theory Comput.* **2019**, 15, 3, 1974–1982.
 - 38) a) Thakur, A.C.; Remsing, R.C. Molecular Structure, Dynamics, and Vibrational Spectroscopy of the Acetylene-Ammonia (1:1) Plastic Co-Crystal at Titan Conditions. *ACS Earth Space Chem.* **2023**, 7, 2, 479–489. b) Thakur, A.C.; Remsing, R.C. Nuclear quantum effects in the acetylene:ammonia plastic co-crystal. *J. Chem. Phys.* **2024** 160, 024502.
 - 39) Yashonath, S.; Rao, C.N.R. Plastic and glassy crystalline states of methane: A Monte Carlo simulation study. *Chem. Phys. Lett.* **1983**, 101, 6, 524–527
 - 40) Choi, K. Y.; Duyker, S. G.; Maynard-Casely, H. E.; Kennedy, B. J. Phase trapping in acetonitrile, a metastable mineral for Saturn's moon Titan. *ACS Earth Space Chem.* **2020**, 4, 8, 1324–1331.
 - 41) Moreau, F.; da Silva, I.; Al Smail, N. et al. Unravelling exceptional acetylene and carbon dioxide adsorption within a tetra-amide functionalized metal-organic framework. *Nat. Commun.* **2017**, 8, 14085.

□